

Synthesis, Structure, and Reactivity of the Methoxy-Bridged Dimer [Cp[∧]Ru(μ-OMe)]₂ (Cp[∧] = η⁵-1-Methoxy-2,4-di-*tert*-butyl-3-neopentylcyclopentadienyl)

Barnali Dutta, Rosario Scopelliti, and Kay Severin*

Institut des Sciences et Ingénierie Chimiques, École Polytechnique Fédérale de Lausanne (EPFL), CH-1015 Lausanne, Switzerland

Received October 4, 2007

The methoxy-bridged Ru^{II} complex [Cp[∧]Ru(μ-OMe)]₂ (Cp[∧] = η⁵-1-methoxy-2,4-di-*tert*-butyl-3-neopentylcyclopentadienyl) was obtained from the Ru^{III} complex [Cp[∧]RuCl(μ-Cl)]₂ by reaction with K₂CO₃ in methanol. In the presence of EtOH, the complex was converted into the ethoxy-bridged dimer [Cp[∧]Ru(μ-OEt)]₂. Due to the steric demand of the Cp[∧] π-ligand, complex [Cp[∧]Ru(μ-OMe)]₂ behaves differently than the parent complex [Cp^{*}Ru(μ-OMe)]₂. Reaction with Me₃SiCl in the presence of LiCl gave the electronically unsaturated complex [Cp[∧]Ru(μ-Cl)]₂, whereas a tetrameric structure had been reported for the analogous Cp^{*} complex. In contrast to the expected addition reaction, a monomeric complex [Cp[∧]Ru(CO)₂(CO₂Me)] was obtained by ligand insertion of CO in the Ru–OMe bond. Moreover, an unprecedented transformation of cyclooctadiene into ethylbenzene in the coordination sphere of Ru was observed. Complex [Cp[∧]Ru(μ-OMe)]₂ was found to act as a highly active catalyst for atom transfer radical cyclization (ATRC) reactions on a diverse range of substrates such as N-substituted dichloro- and trichloroacetamides, enamides, ethers, and esters.

Introduction

Ruthenium half-sandwich complexes have found numerous applications as catalysts for organic transformations¹ but also in the field of supramolecular² and medicinal chemistry.³ Apart from (arene)Ru complexes, compounds based on the Cp^{*}Ru fragment have received considerable interest in this context. A particularly useful starting material for the organometallic chemistry of Cp^{*}Ru complexes turned out to be the methoxy-bridged dimer [Cp^{*}Ru(μ-OMe)]₂.^{4,5} This complex, which is available in two steps from RuCl₃(H₂O)_n,⁶ is air-sensitive but thermally stable under an inert atmosphere. It rapidly undergoes addition as well as substitution reactions. The versatile reactivity

of this species has been attributed to the electronically unsaturated Ru centers and due to the lability and basicity of the methoxy ligands.⁴

Recently, we have reported the synthesis of the Ru^{III} complex [Cp[∧]RuCl(μ-Cl)]₂ (Cp[∧] = 1-methoxy-2,4-di-*tert*-butyl-3-neopentylcyclopentadienyl), which can easily be obtained by reaction of RuCl₃(solvent)_n with *tert*-butyl acetylene.⁷ First investigations had shown that the dimeric Ru^{III} complex [Cp[∧]RuCl(μ-Cl)]₂ can be transformed into mononuclear Ru^{II} complexes.⁸ In view of the synthetic importance of the methoxy-bridged dimer [Cp^{*}Ru(μ-OMe)]₂, we attempted to prepare the analogous Cp[∧] complex [Cp[∧]Ru(μ-OMe)]₂ (**1**). Below we describe the chemistry of this complex. It was found that the sterically demanding Cp[∧] ligand leads to unique structures as well as to a distinct reactivity in stoichiometric and catalytic transformations.

Results and Discussion

Following a synthetic pathway described for [Cp^{*}Ru(μ-OMe)]₂,^{6c} we were able to obtain complex [Cp[∧]Ru(μ-OMe)]₂ (**1**) in good yield (70%) by stirring [Cp[∧]RuCl(μ-Cl)]₂ in MeOH in the presence of K₂CO₃ (Scheme 1). Complex **1** was found to be very air-sensitive and well-soluble in nonpolar organic solvents. The ¹H NMR spectrum of **1** in CD₂Cl₂ showed the presence of two diastereoisomers, in a ratio of 1:1, arising due to the planar chirality of the Cp[∧] ligand.

Orange crystals of complex **1** were obtained from a hexane solution by slow evaporation. A crystallographic analysis revealed that the *meso* diastereomer with opposite configuration of the two Cp[∧]Ru fragments had crystallized (Figure 1). Although the overall structure of complex **1** is analogous to

* Corresponding author. E-mail: kay.severin@epfl.ch.

(1) (a) Trost, B. N.; Frederiksen, M. U.; Rudd, M. T. *Angew. Chem., Int. Ed.* **2005**, *44*, 6630–6666. (b) Murahashi, S. I. *Ruthenium in Organic Synthesis*; Wiley-VCH: Weinheim, 2004. (c) Bruneau, C.; Dixneuf, P. H. *Ruthenium Catalysts and Fine Chemistry*; Springer: Berlin, 2004. (d) Dérien, S.; Dixneuf, P. H. *J. Organomet. Chem.* **2004**, *689*, 1382–1392. (e) Trost, B. M.; Toste, F. D.; Pinkerton, A. B. *Chem. Rev.* **2001**, *101*, 2067–2096. (f) Naota, T.; Takaya, H.; Murahashi, S. I. *Chem. Rev.* **1998**, *98*, 2599–2660.

(2) Severin, K. *Chem. Commun.* **2006**, 3859–3867.

(3) (a) Ang, W. H.; Dyson, P. J. *Eur. J. Inorg. Chem.* **2006**, 4003–4018. (b) Melchart, M.; Sadler, P. J. In *Bioorganometallics*; Jaouen, G., Ed.; Wiley-VCH: Weinheim, 2006; pp 39–62. (c) Allardyce, C. S.; Dorcier, A.; Scolaro, C.; Dyson, P. J. *Appl. Organomet. Chem.* **2005**, *19*, 1–10.

(4) For a review see Koelle, U. *Chem. Rev.* **1998**, *98*, 1313–1334.

(5) (a) For some selected recent applications see: Murphy, J. M.; Lawrence, J. D.; Kawamura, K.; Incarvito, C.; Hartwig, J. F. *J. Am. Chem. Soc.* **2006**, *128*, 13684–13685. (b) Quebatte, L.; Scopelliti, R.; Severin, K. *Eur. J. Inorg. Chem.* **2006**, 231–236. (c) Ito, J.; Shima, T.; Suzuki, H. *Organometallics* **2006**, *25*, 1333–1336. (d) Kuan, S. L.; Leong, W. K.; Goh, L. Y.; Webster, R. D. *J. Organomet. Chem.* **2006**, *691*, 907–915. (e) Shima, T.; Suzuki, H. *Organometallics* **2005**, *24*, 3939–3945. (f) Chaumonnot, A.; Donnadiou, B.; Sabo-Etienne, S.; Chaudret, B.; Buron, C.; Bertrand, G.; Metivier, P. *Organometallics* **2001**, *20*, 5614–5618.

(6) (a) Loren, S. D.; Campion, B. K.; Heyn, R. H.; Tilley, T. D.; Bursten, B. E.; Luth, K. W. *J. Am. Chem. Soc.* **1989**, *111*, 4712–4718. (b) Koelle, U.; Kossakowski, J. *J. Organomet. Chem.* **1989**, *362*, 383–398. (c) Koelle, U.; Kossakowski, J. *Chem. Commun.* **1988**, 549–551.

(7) Gauthier, S.; Solari, E.; Dutta, B.; Scopelliti, R.; Severin, K. *Chem. Commun.* **2007**, 1837–1839.

(8) Dutta, B.; Solari, E.; Gauthier, S.; Scopelliti, R.; Severin, K. *Organometallics* **2007**, *26*, 4791–4799.

Scheme 1

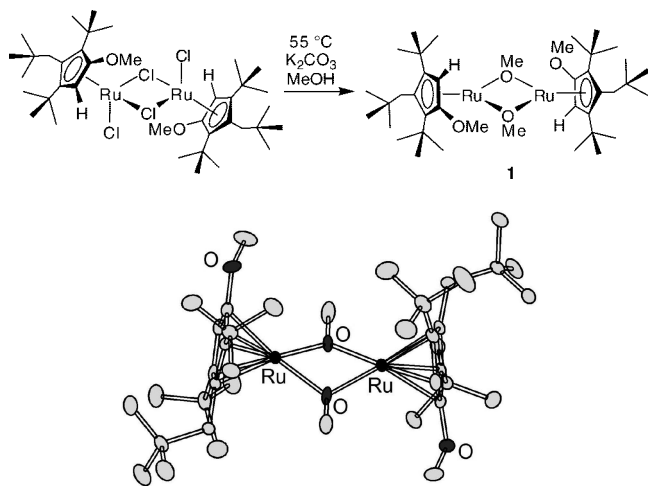


Figure 1. Graphic representation of the molecular structure of complex **1** in the crystal. Thermal ellipsoids are at the 50% probability level. Hydrogen atoms are not shown for clarity.

Scheme 2

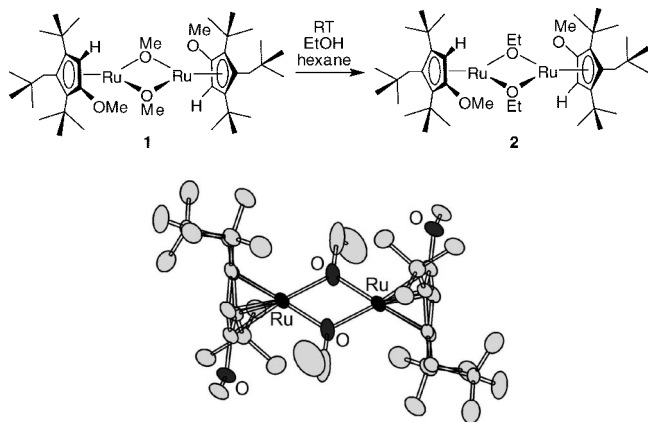


Figure 2. Graphic representation of the molecular structure of complex **2** in the crystal. Thermal ellipsoids are at the 50% probability level. The hydrogen atoms are not shown for clarity.

that of $[\text{Cp}^*\text{Ru}(\mu\text{-OME})_2]$, there are notable variations in certain interatomic distances and bond angles (Table 1). The average Ru–O and O–CH₃ bond distances are similar to what has been reported for $[\text{Cp}^*\text{Ru}(\mu\text{-OME})_2]$,^{6a} but the spatial separation of the Ru centers is higher in complex **1** (3.2944(7) Å as compared to 2.961(1) Å for the Cp* analogue). The average Ru–O–Ru bond angle in complex **1** (103.89°) is also significantly higher than that in $[\text{Cp}^*\text{Ru}(\mu\text{-OME})_2]$ (91.5(1)°). Furthermore, the Ru₂O₂ core of **1** is only slightly bent along the O···O axis (fold angle = 157.1°), whereas the Cp*Ru dimer is strongly folded (fold angle = 124.3°). It is presumed that these differences are a manifestation of the increased steric demand of the Cp[^] ligand compared to the Cp* ligand. The overcrowding arising from the bulky alkyl groups on the Cp[^] is balanced by means of a longer Ru···Ru distance and increased Ru–O–Ru angles.

For complex $[\text{Cp}^*\text{Ru}(\mu\text{-OME})_2]$ it has been reported that the methoxy ligands can easily be exchanged for ethoxy ligands. In analogy, the $\mu\text{-OEt}$ complex **2** was obtained in 94% yield by slow diffusion of ethanol into a solution of complex **1** in hexane. The structure of **2** was established by single-crystal X-ray analysis, NMR spectroscopy and elemental analysis. As

Table 1. Selected Distances (Å) and Angles (deg) for the Complexes **1**, $[\text{Cp}^*\text{Ru}(\mu\text{-OME})_2]$, and **2**

	1 ^a	$[\text{Cp}^*\text{Ru}(\mu\text{-OME})_2]$ ^b	2
Ru···Ru	3.294(1)	2.961(1)	3.370(4)
Ru–O	2.092	2.067(2)	2.066
O–C _{Me/Et}	1.385	1.389(4)	1.435(10)
Ru–O–Ru	103.89	91.5(1)	109.2(2)
O–Ru–O	73.07	71.8(1)	70.8(2)
Ru–O–C _{Me/Et}	126.05	124.7(2)	125.05

^a Averaged values are given. ^b Data from ref 6a.

it was observed for complex **1**, the ¹H NMR spectrum revealed the existence of two diastereoisomers in the ratio of 1:1 in solution.

The structural analysis of **2** showed the presence of a crystallographic inversion center. The Ru₂O₂ core is thus perfectly flat. As a consequence, the Ru···Ru distance in **2** is larger than that in **1** (3.370(4) Å) and the Ru–O–Ru angle is larger (109.2(2)°). In other respects the structure of complex **2** is similar to **1**. Key structural features of **2** are summarized in Table 1.

Another widely used starting material for the synthesis of Cp*Ru^{II} half-sandwich complexes is $[\text{Cp}^*\text{Ru}(\mu\text{-Cl})_4]$.⁹ It can be obtained by reduction of $[\text{Cp}^*\text{RuCl}(\mu\text{-Cl})_2]$ with LiHBt₃¹⁰ or with Zn.¹¹ Alternatively, it can be synthesized by reaction of $[\text{Cp}^*\text{Ru}(\mu\text{-OME})_2]$ with Me₃SiCl and LiCl.^{6b,c} To generate the analogous Cp[^] complex, we opted for the latter route. Addition of Me₃SiCl to a THF solution of **1** did not result in any visible change, even upon heating to 65 °C. When LiCl was added, however, the equilibrium shifted to the product $[\text{Cp}^*\text{Ru}(\mu\text{-Cl})_2]$ (**3**), as indicated by a color change from orange-yellow to red (Scheme 3). After 12 h, the excess of Me₃SiCl and the lithium salts were removed to give complex **3** as a reddish-brown solid, which was very air-sensitive (yield: 88%).

Single crystals of complex **3** were obtained from a CH₂Cl₂/MeOH solution at –35 °C. A crystallographic analysis revealed that the structure of **3** was again very distinct from that of its Cp* analogue: whereas a tetramer with a distorted heterocubane structure was reported for $[\text{Cp}^*\text{Ru}(\mu\text{-Cl})_4]$,¹² complex **3** showed a dimeric structure with two bridging chloride ligands (Figure 3).

As it was observed for the alkoxy-bridged dimers **1** and **2**, it was the *meso* diastereoisomer that had crystallized. In solution, however, the presence of two diastereoisomers in the ratio of 1:2 was detected by ¹H NMR spectroscopy. The solid state structure of complex **3** shows a Ru···Ru separation of 3.6023(5) Å and hence no intermetallic interaction. The average Ru–Cl distance in **3**, 2.4351 Å, is smaller than that in $[\text{Cp}^*\text{Ru}(\mu\text{-Cl})_4]$ (2.5244 Å).¹² The average Ru–Cl–Ru and Cl–Ru–Cl bond

(9) (a) For some selected recent applications see: Miyake, Y.; Nomaguchi, Y.; Yuki, M.; Nishibayashi, Y. *Organometallics* **2007**, *26*, 3611–3613. (b) Hoover, J. M.; DiPasquale, A.; Mayer, J. M.; Michael, F. A. *Organometallics* **2007**, *26*, 3297–3305. (c) Fairchild, R. M.; Holman, K. T. *Organometallics* **2007**, *26*, 3049–3053. (d) Tokitoh, N.; Nakata, N.; Shinohara, A.; Takeda, N.; Sasamori, T. *Chem. Eur. J.* **2007**, *13*, 1856–1862. (e) Zheng, W.; Zhang, G.; Fan, K. *Organometallics* **2006**, *25*, 1548–1550. (f) Fukumoto, H.; Mashima, K. *Eur. J. Inorg. Chem.* **2006**, 5006–5011. (g) Dysard, J. M.; Tilley, T. D. *Organometallics* **2000**, *23*, 4726–4732. (h) Koelle, U.; Kang, B. S.; Englert, U. *J. Organomet. Chem.* **1991**, *420*, 227–235. (i) Campion, B. K.; Heyn, R. H.; Tilley, T. D. *Organometallics* **1990**, *9*, 1106–1112.

(10) Fagan, P. J.; Ward, M. D.; Calabrese, J. C. *J. Am. Chem. Soc.* **1989**, *111*, 1698–719.

(11) (a) Chaudret, B.; Jalón, F.; Perez-Manrique, M.; Lahoz, F.; Plou, F. J.; Sanchez-Delgado, R. *New J. Chem.* **1990**, *14*, 331–8. (b) Chaudret, B.; Jalón, F. A. *J. Chem. Soc., Chem. Commun.* **1988**, 711–713.

(12) Fagan, P. J.; Mahoney, W. S.; Calabrese, J. C.; Williams, I. D. *Organometallics* **1990**, *9*, 1843–1852.

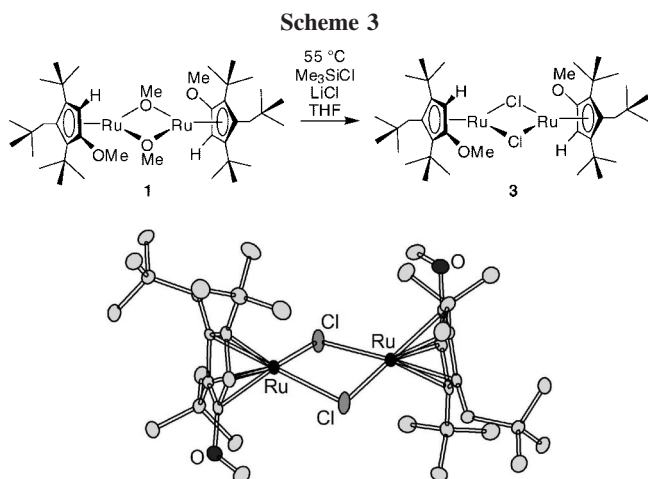
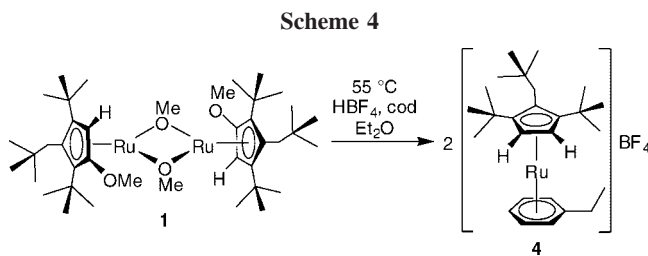


Figure 3. Graphic representation of the molecular structure of complex **3** in the crystal. The hydrogen atoms are not shown for clarity. Selected bond lengths (Å) and angles (deg): Ru–Ru 3.6023(5), Ru–Cl 2.4351; Ru–Cl–Ru 95.40, Cl–Ru–Cl 82.74.



angles are 95.40° and 82.74° , respectively, and the Ru_2Cl_2 core is only slightly bent (fold angle = 160.50°).

The fact that complex **3** forms a dinuclear structure instead of a tetranuclear one is likely a consequence of the sterically demanding Cp^* ligand. It is a further evidence that the Cp^* allows access to electronically unsaturated complexes, which are not accessible with the classical Cp^* ligand.⁸ Overall, the crystallographic studies described above show that the Cp^* ligand may have a pronounced influence on the structures of the complexes. Below we demonstrate that the reactivity can be strongly affected as well.

The reaction of $[\text{Cp}^*\text{Ru}(\mu\text{-OMe})]_2$ with acids such as $\text{CF}_3\text{SO}_3\text{H}$ is known to result in the formation of the highly reactive Cp^*Ru^+ cation, which displays useful chemical properties. Due to the high affinity of the Cp^*Ru^+ species for six-electron donor ligands, the generation of $\eta^6 \pi$ -ligands by C–H, C–O, and C–C activation reactions can be observed. Examples include the aromatization of six-membered cyclic alkenes, ketones, and enones.¹³ When Cp^*Ru^+ was reacted with 1,5-cyclooctadiene (cod), both Singleton and Chaudret observed the formation of the η^6 -1,3,5-cyclooctatriene cation $[\text{Cp}^*\text{Ru}(\text{C}_8\text{H}_{10})]^+$ by dehydrogenation of cod.¹⁴ When we examined a similar reaction with $[\text{Cp}^*\text{Ru}(\mu\text{-OMe})]_2$ (**1**), we obtained a surprising result: instead of the analogous $[\text{Cp}^*\text{Ru}(\text{C}_8\text{H}_{10})]^+$,

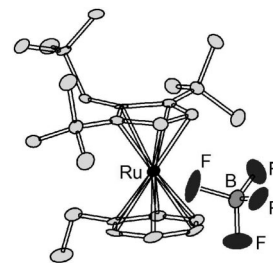


Figure 4. Graphic representation of the molecular structure of complex **4** in the crystal. The hydrogen atoms are not shown for clarity.

we observed the nearly quantitative formation (isolated yield: 87%) of the η^6 -ethylbenzene complex **4** (Scheme 4). The structure of **4** was evidenced by NMR spectroscopy, elemental analysis, and single-crystal X-ray analysis (Figure 4).

The first thing to notice is the change of the methoxy-substituted Cp^* ligand into a η^5 -1,3-di-*tert*-butyl-2-neopentyl-cyclopentadienyl ligand. Furthermore, cod had transformed into Ru-bound ethylbenzene. Instead of a simple dehydrogenation reaction, an additional C–C activation reaction had thus taken place. A mechanism might involve a rearrangement of an intermediate cyclooctatriene into bicyclo[4.2.0]octa-2,4-diene and thereafter a C–C bond activation leading to the ethylbenzene ligand. The existence of a dynamic equilibrium between 1,3,5-cyclooctatriene and bicyclo[4.2.0]octa-2,4-diene (valence tautomerism) has been reported already in 1952.¹⁵ The driving force behind the final aromatization would be the favorable coordination of the $\eta^6 \pi$ -ligand, ethylbenzene, to the Ru center, forming an $18 e^-$ sandwich complex. To the best of our knowledge such a Ru-induced transformation of cod into ethylbenzene is unprecedented.

Another transformation in which the methoxy-bridged complex **1** displayed a very distinct reactivity was the reaction with carbon monoxide. When CO was passed into a hexane solution of complex **1**, the solution slowly turned yellow, and on standing at low temperature yellow crystals gradually appeared. The analytical data showed that the monomeric complex **5** had formed in quantitative yield as a result of the insertion of CO into the Ru–OMe bond (Scheme 5). In contrast, the reaction of the Cp^* analogue $[\text{Cp}^*\text{Ru}(\mu\text{-OMe})]_2$ with 1 atm CO was reported to give the dimer $[\text{Cp}^*\text{Ru}(\text{CO})(\mu\text{-CO})]_2$, presumably via the simple addition product $[\text{Cp}^*\text{Ru}(\text{CO})(\mu\text{-OMe})]_2$.⁶ A complex of the latter type had been isolated using $[\text{Cp}^*\text{Ru}(\mu\text{-OEt})]_2$ instead of $[\text{Cp}^*\text{Ru}(\mu\text{-OMe})]_2$.^{6a} It should be noted, however, that the Cp^* analogue of **5** can be prepared by the attack of methoxide anion on the tricarbonyl complex $[\text{Cp}^*\text{Ru}(\text{CO})_3]\text{BF}_4$.¹⁶

Complex **5** was characterized by IR and NMR spectroscopy as well as by elemental analysis. The CO stretching frequencies of **5** ($\nu_{\text{CO}} = 2017$ and 1957 cm^{-1}) were found to be lower than that of $[\text{Cp}^*\text{Ru}(\text{CO})_2(\text{COOMe})]$ ($\nu_{\text{CO}} = 2022$ and 1961 cm^{-1}).¹⁶ This implies a slightly better electron back-donation from Ru and thus a higher electron-donating ability of the Cp^* ligand compared to Cp^* .

The structure of complex **5** was also confirmed by single-crystal X-ray crystallography. The structural analysis showed Ru–C distances for the terminal CO ligands of 1.886(2) and 1.888(3) Å, while the acyl Ru–C bond length was 2.083(2) Å.

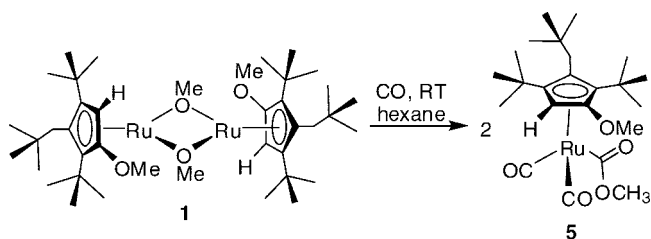
(13) (a) Urbanos, F.; Halcrow, M. A.; Fernandez-Baeza, J.; Dahan, F.; Labroue, D.; Chaudret, B. *J. Am. Chem. Soc.* **1993**, *115*, 3484–3493. (b) Carreno, R.; Chaudret, B.; Labroue, D.; Sabo-Etienne, S. *Organometallics* **1993**, *12*, 13–14. (c) Halcrow, M. A.; Urbanos, F.; Chaudret, B. *Organometallics* **1993**, *12*, 955–957. (d) Huang, Y.; Sabo-Etienne, S.; He, X. D.; Chaudret, B. *Organometallics* **1992**, *11*, 3031–3035. (e) Chaudret, B.; Dahan, F.; He, X. D. *Chem. Commun.* **1990**, 1111–1113.

(14) (a) Rondon, D.; Chaudret, B.; He, X. D.; Labroue, D. *J. Am. Chem. Soc.* **1991**, *113*, 5671–5676. (b) Albers, M. O.; Liles, D. C.; Robinson, D. J.; Singleton, E. *Chem. Commun.* **1986**, 1102–1104.

(15) Cope, A. C.; Haven, A. C.; Ramp, F. L.; Trumbull, E. R. *J. Am. Chem. Soc.* **1952**, *74*, 4867–4871.

(16) Suzuki, H.; Omori, H.; Moro-oka, Y. *J. Organomet. Chem.* **1987**, *327*, C47–C50.

Scheme 5



The C–Ru–C bond angle involving the terminal carbonyls was found to be $89.69(10)^\circ$, and the C–Ru–C angles involving the acyl CO and a terminal CO are $87.01(9)^\circ$ and $91.84(10)^\circ$, respectively.

In addition to reactivity studies, we have investigated the catalytic activity of complex **1**. Here, we focused on atom transfer radical cyclization (ATRC) reactions, which can be regarded as intramolecular versions of the Kharasch addition.¹⁷ ATRC reactions are versatile C–C coupling reactions, which are increasingly being used in organic synthesis.^{18,19} Ruthenium and copper complexes are frequently used as catalysts for this type of reaction. Of particular interest for the present study was the fact that the Cp* analogue of complex **1**, [Cp*Ru(μ -OMe)]₂, is one of the most active Ru-based catalysts described so far.^{20,21}

First we investigated the cyclization of *N*-allyl-*N*-tosyldichloroacetamide (**6**) to give the corresponding γ -lactam **7** (Scheme 6). The amide **6** is not a particularly active ATRC substrate and [Cp*Ru(OMe)]₂ is one of the few complexes that is able to catalyze this reaction at ambient temperatures.²⁰ To evaluate the catalytic activity of complex **1**, we have investigated the time course of the reaction catalyzed by 5 mol % (10 mol % Ru) of either **1** or [Cp*Ru(μ -OMe)]₂ by NMR spectroscopy. One equivalent of pyridine with respect to the dimer was added because it had been reported that pyridine accelerates the catalytic rate of [Cp*Ru(μ -OMe)]₂.²⁰

The time courses of the reactions are depicted in Figure 6. The cyclization of amide **6** with the catalyst [Cp*Ru(μ -OMe)]₂ gave a yield of 86% after 150 min. For the new complex **1**, a similar yield was observed after only 20 min, indicating a substantial increase in catalytic activity. The trans/cis ratio of the product was in both cases approximately 87:13 as determined by ¹H NMR. The high catalytic activity of **1** allowed performing

(17) (a) Severin, K. *Curr. Org. Chem.* **2006**, *10*, 217–224. (b) Delaude, L.; Demonceau, A.; Noels, A. F. *Top. Organomet. Chem.* **2004**, *11*, 155–171.

(18) (a) For reviews see: Clarke, A. J. *Chem Soc Rev.* **2002**, *31*, 1–11. (b) Matyjaszewski, K. *Curr. Org. Chem.* **2002**, *6*, 67–82. (c) Iqbal, J.; Bhatia, B.; Nayyar, N. K. *Chem. Rev.* **1994**, *94*, 519–564. (d) Minisci, F. *Acc. Chem. Res.* **1975**, *8*, 165–171.

(19) (a) For selected recent examples see: Bull, J. A.; Hutchings, M. G.; Quayle, P. *Angew. Chem., Int. Ed.* **2007**, *46*, 1869–1872. (b) Bellesia, F.; Danieli, C.; De Buyck, L.; Galeazi, R.; Ghelfi, F.; Mucci, A.; Orena, M.; Pagnoni, U. M.; Parsons, A. F.; Roncaglia, F. *Tetrahedron* **2006**, *62*, 746–757. (c) De Buyck, L.; Forzato, C.; Ghelfi, F.; Mucci, A.; Nitti, P.; Pagnoni, U. M.; Parson, A. F.; Pitocco, G.; Roncaglia, F. *Tetrahedron Lett.* **2006**, *47*, 7759–7762. (d) Edlin, C. D.; Faulkner, J.; Helliwell, M.; Knight, C. K.; Parker, J.; Quayle, P.; Raftery, J. *Tetrahedron* **2006**, *62*, 3004–3015. (e) Seigal, B. A.; Fajardo, C.; Snapper, M. L. *J. Am. Chem. Soc.* **2005**, *127*, 16329–16332. (f) Schmidt, B.; Pohler, M. *J. Organomet. Chem.* **2005**, *690*, 5552–5555.

(20) Motoyama, Y.; Hanada, S.; Shimamoto, K.; Nagashima, H. *Tetrahedron* **2006**, *62*, 2779–2788.

(21) (a) For other highly active Ru catalysts see: Thommes, K.; Içli, B.; Scopelliti, R.; Severin, K. *Chem. Eur. J.* **2007**, *13*, 6899–6907. (b) Motoyama, Y.; Hanada, S.; Niibayashi, S.; Shimamoto, K.; Takaoka, N.; Nagashima, H. *Tetrahedron* **2005**, *61*, 10216–10226. (c) Motoyama, Y.; Gondo, M.; Masuda, S.; Iwashita, Y.; Nagashima, H. *Chem. Lett.* **2004**, *33*, 442–443. (d) Nagashima, H.; Gondo, M.; Masuda, S.; Kondo, H.; Yamaguchi, Y.; Matsubara, K. *Chem. Commun.* **2003**, 442–443.

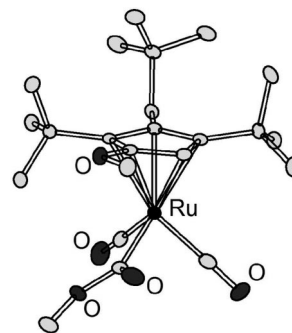


Figure 5. Graphic representation of the molecular structure of complex **5** in the crystal. The hydrogen atoms are not shown for clarity. Selected bond lengths (Å): Ru–CO_{terminal} 1.886(2), 1.888(3), Ru–COOMe 2.083(2).

the reaction at 0 °C: a yield of 90% was achieved after 150 min using 5 mol % of **1**. Lowering the catalyst concentration to 2.5 mol % at room temperature resulted in a slightly lower yield of 75% after 150 min.

The very promising results obtained for the benchmark reaction with substrate **6** prompted us to investigate other ATRC reactions. Cyclizations of *N*-allyl-*N*-alkyltrichloroacetamides have been studied widely in the groups of Itoh and Nagashima, among others.²² These ATRC reactions can be performed with 5 mol % of RuCl₂(PPh₃)₃ or 30 mol % of CuCl/bipy at elevated temperatures. Ruthenium complexes with amidinate ligands are known to catalyze such reactions at room temperature, but high catalyst loadings (10–20 mol % Ru) are required.^{21b,d} We were able to perform the cyclization of *N*-allyl-*N*-phenyltrichloroacetamide (**8**) with 2.5 mol % of complex **1**/pyridine (5 mol % Ru) at RT to give the product **9** in 88% yield after 3 h (Table 2, entry 1). With a higher catalyst loading (5 mol % **1**) the reaction was found to be complete almost instantaneously, giving a yield of 90% within 10 min.

The ATRC of α -bromo enamides has been studied by Clarke et al.²³ They found that the cyclization of **10** can be carried out in good yield using CuBr (30 mol%) along with the activating ligand tris(*N,N*-2-dimethylamino)ethylamine (30 mol %). It was suggested that **10** undergoes a 5-*endo* cyclization to give a mixture of the γ -lactams **11a** and **11b** through a radical-polar crossover mechanism with elimination of HBr.^{23c} Using the Ru catalyst **1**, it is possible to perform the reaction at room temperature with a catalyst concentration of only 0.25 mol % (Table 2, entry 2).

Transition-metal-catalyzed ATRC reactions of polyoxalkenyl trichloroesters have been investigated by Verlhac et al.²⁴ Cu^I and Fe^{II} complexes (10 mol %) were employed at 80 °C to promote the cyclization of 2-(allyloxy)ethyl-2,2,2-trichloroacetate **12**. Reactions catalyzed by FeCl₂/N¹-[2-(dimethylamino)ethyl]-N¹,N²,N²-trimethylethane-1,2-diamine gave **13** in 56% yield, while the Cu catalysts resulted in poor yields. We

(22) (a) Nagashima, H.; Ozaki, N.; Ishii, M.; Seki, K.; Washiyama, M.; Itoh, K. *J. Org. Chem.* **1993**, *58*, 464–470. (b) Nagashima, H.; Wakamatsu, H.; Ozaki, N.; Ishii, T.; Watanabe, M.; Tajima, T.; Itoh, K. *J. Org. Chem.* **1992**, *57*, 1682–1689. (c) Nagashima, H.; Ozaki, N.; Seki, K.; Ishii, M.; Itoh, K. *J. Org. Chem.* **1989**, *54*, 4497–4499. (d) Boivin, J.; Yousfi, M.; Zard, S. Z. *Tetrahedron Lett.* **1994**, *35*, 5629–5632. (e) Edlin, C. D.; Faulkner, J.; Quayle, P. *Tetrahedron Lett.* **2006**, *47*, 1145–1151.

(23) (a) Clark, A. J.; Geden, J. V.; Thom, S. *J. Org. Chem.* **2006**, *71*, 1471–1479. (b) Clark, A. J.; Filik, R. P.; Haddleton, D. M.; Radigue, A.; Sanders, C. J.; Thomas, G. H.; Smith, M. E. *J. Org. Chem.* **1999**, *64*, 8954–8957. (c) Clark, A. J.; Dell, C. P.; Ellard, J. M.; Hunt, N. A.; McDonagh, J. P. *Tetrahedron Lett.* **1999**, *40*, 8619–8623.

(24) Campo, F.; Lastécouères, D.; Verlhac, J.-B. *J. Chem. Soc., Perkin Trans. 1* **2000**, 575–580.

Scheme 6

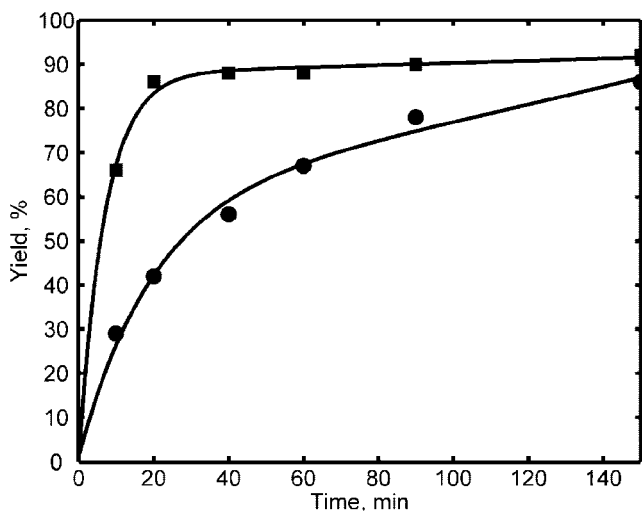
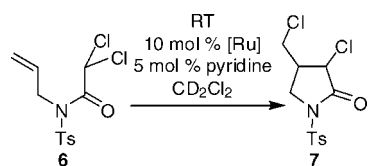


Figure 6. Reaction profiles for the cyclization of **6** catalyzed by [Cp^{*}Ru(μ-OMe)]₂ (●) or by complex **1** (■). Reaction conditions: RT, CD₂Cl₂ (total volume = 1000 μL), [substrate] = 0.15 M, [pyridine] = 7.5 mM, [Ru] = 15 mM. The yield is based on the formation of the product as determined from ¹H NMR spectroscopy using the internal standard *p*-xylene (50 mM).

employed complex **1** at 60 °C with a catalyst concentration of 1.0 mol % and obtained the product in a yield of 65% (Table 2, entry 3).

Studies on ATRC reactions of ethers have been carried out by Ram and Charles.²⁵ They have reported that the cyclization of 2,2,2-trichloroethyl ethers can be achieved using CuCl/bipy (30 mol %) as the catalyst at 80 °C. When complex **1** (2.5 mol %) was used for the ATRC reaction of [(2,2,2-trichloroethoxy)-prop-1-enyl]benzene (**14**), a yield of 60% was obtained at room temperature after 20 h (Table 2, entry 4).

Ruthenium-catalyzed atom transfer radical reactions of halogenated compounds are believed to proceed via the reversible formation of a Ru^{III}X complex from a Ru^{II} complex.¹⁷ A redox pair of this kind is likely to be involved in the ATRC reactions with complex **1**. An interesting question is whether monomeric or dinuclear complexes are present in the catalytic cycle.²⁶ For [Cp^{*}Ru(μ-OMe)]₂ it had been suggested that the role of the pyridine is to stabilize catalytically active monomeric complexes, which are in a dynamic equilibrium with dimeric species.²⁰ A related situation seems plausible for reactions catalyzed by complex **1**, but further mechanistic studies are needed to clarify this point.

Conclusion

We have described the synthesis of the methoxy-bridged dimer [Cp^{*}Ru(μ-OMe)]₂ (**1**), an analogue of the frequently used

Table 2. ATRC Reactions Catalyzed by Complex **1**^a

Entry	Substrate	Product	[1] [mol%]	<i>t</i> [h]	<i>T</i> [°C]	Conv. ^c [%]	Yield ^d [%]
1			2.5	3.0	RT	94	88
2 ^b		 	0.25	20	RT	82	78 (33:67)
3			1.0	48	60	91	65
4			2.5	20	RT	70	60 (86:14)

^a The reactions were performed in *d*₈-toluene (total volume = 1000 μL, [substrate] = 0.15 M) using 1 equiv of pyridine with respect to catalyst **1**. ^b One equivalent of NEt₃ with respect to the substrate was added to the reaction mixture. ^c The conversion is based on the consumption of the olefin and the yield is based on the formation of the product as determined by ¹H NMR spectroscopy using 1,4-bis(trifluoromethyl)benzene (50 mM) as the internal standard.

starting material [Cp^{*}Ru(μ-OMe)]₂. Complex **1** turned out to display a distinct chemistry, from both a structural and reactivity point of view. In the solid state, complex **1** shows only a slightly bent structure with a Ru···Ru distance of 3.2944(7) Å, whereas the Ru₂O₂ core of [Cp^{*}Ru(μ-OMe)]₂ is strongly folded with a metal–metal distance of less than 3 Å. The reaction with cod in the presence of HBF₄ resulted in an unprecedented dehydrogenation and rearrangement of cod to give a η⁶-ethylbenzene sandwich complex, and the reaction with CO led to the formation of the monomeric complex [Cp^{*}Ru(CO)₂(COOMe)] instead of a dimeric carbonyl complex as observed for [Cp^{*}Ru(μ-OMe)]₂. When the methoxy ligands in **1** were replaced by chloro ligands, the resulting complex **3** displayed a dimeric structure, whereas a tetramer was observed for the corresponding Cp^{*} complex. Complex **1** can be used as a catalyst precursor for ATRC reactions of amides, esters, and ethers. Kinetic studies with the substrate *N*-allyl-*N*-tosyldichloroacetamide have shown that its activity surpasses that of complex [Cp^{*}Ru(μ-OMe)]₂.

The unique chemistry of complex **1** can be attributed to the pronounced steric demand of the Cp^{*} ligand. It is expected that interesting differences in structure and reactivity will also be observed for other Cp^{*}Ru complexes. Further research along these lines should be stimulated by the fact that synthetically useful precursors such as **1** and [Cp^{*}Ru(μ-Cl)]₂ (**3**) are easily accessible.

Experimental Section

General Comments. All experiments were performed inside a glovebox under an atmosphere of dinitrogen containing less than 1 ppm of oxygen and water. Thoroughly dried and deoxygenated solvents were used. RuCl₃(H₂O)_{*n*} was obtained from Precious Metals Online. Me₃SiCl, LiCl (anhydrous), K₂CO₃, and cod were purchased from Fluka. All chemicals were used as received, unless otherwise stated. ¹H and ¹³C spectra were recorded on a Bruker Advance DPX 400 spectrometer using deuterated solvents. The deuterated solvents CD₂Cl₂ and C₆D₅CD₃ (from Aldrich) for NMR experiments were degassed by three freeze–pump–thaw cycles and

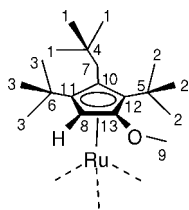
(25) Ram, R. N.; Charles, I. *Chem. Commun.* **1999**, 2267–2268.

(26) (a) For atom transfer radical reactions with dinuclear catalyst precursors see refs 20, 21b, 21c and : Haas, M.; Solari, E.; Nguyen, Q. T.; Gauthier, S.; Scopelliti, R.; Severin, K. *Adv. Synth. Catal.* **2006**, *348*, 439–442. (b) Quebatte, L.; Solari, E.; Scopelliti, R.; Severin, K. *Organometallics* **2005**, *24*, 1404–1406. (c) Quebatte, L.; Scopelliti, R.; Severin, K. *Angew. Chem., Int. Ed.* **2004**, *43*, 1520–1524. (d) de Clercq, B.; Verpoort, F. *Tetrahedron Lett.* **2002**, *43*, 4687–4690.

Table 3. Crystallographic Data for Complexes 1, 2, and 3

	1	2	3
empirical formula	C ₄₀ H ₇₂ O ₄ Ru ₂	C ₄₂ H ₇₆ O ₄ Ru ₂	C ₃₈ H ₆₆ Cl ₂ O ₂ Ru ₂
mol wt/g mol ⁻¹	819.12	847.17	827.95
cryst size/mm ³	0.84 × 0.63 × 0.49	0.43 × 0.23 × 0.15	0.25 × 0.16 × 0.13
cryst syst	orthorhombic	triclinic	triclinic
space group	<i>Pca</i> 2 ₁	<i>P</i> 1	<i>P</i> 1
<i>a</i> /Å	12.0703(16)	8.866(11)	11.0340(10)
<i>b</i> /Å	17.266(3)	10.418(4)	13.1061(13)
<i>c</i> /Å	19.3130(15)	12.367(10)	14.4173(12)
<i>α</i> /deg	90	71.30(5)	70.663(9)
<i>β</i> /deg	90	76.30(12)	89.125(7)
<i>γ</i> /deg	90	80.89(7)	84.057(7)
volume/Å ³	4025.0(8)	1047.0(16)	1956.3(3)
Z	4	1	2
density/g cm ⁻³	1.352	1.344	1.406
temperature/K	100(2)	100(2)	100(2)
absorp coeff/mm ⁻¹	0.787	0.758	0.938
<i>θ</i> range/deg	3.38 to 25.03	3.54 to 25.03	3.31 to 25.03
index ranges	-14 → 14, -20 → 20, -22 → 22	-10 → 10, -12 → 12, -14 → 14	-13 → 13, -15 → 15, -17 → 16
no. of reflns collected	46632	19229	39214
no. of indep reflns	6714 (<i>R</i> _{int} = 0.0411)	3671 (<i>R</i> _{int} = 0.0816)	6885 (<i>R</i> _{int} = 0.0512)
absorp corr	semiempirical	semiempirical	semiempirical
max. and min. transm	1.0000 and 0.8690	1.0000 and 0.4260	1.0000 and 0.7726
no. of data/restraints/params	6714/1/417	3671/1/217	6885/0/397
goodness-of-fit on <i>F</i> ²	1.146	1.033	1.230
final <i>R</i> indices [<i>I</i> > 2σ(<i>I</i>)]	<i>R</i> 1 = 0.0240, <i>wR</i> 2 = 0.0485	<i>R</i> 1 = 0.0651, <i>wR</i> 2 = 0.1651	<i>R</i> 1 = 0.0357, <i>wR</i> 2 = 0.0712
<i>R</i> indices (all data)	<i>R</i> 1 = 0.0315, <i>wR</i> 2 = 0.531	<i>R</i> 1 = 0.0740, <i>wR</i> 2 = 0.1755	<i>R</i> 1 = 0.0511, <i>wR</i> 2 = 0.0764
larg diff peak/hole/e Å ⁻³	0.383 and -0.576	1.622 and -0.968	0.841 and -0.556

then purified by vacuum transfer at room temperature. IR spectra were recorded on a Perkin-Elmer FT-IR spectrometer. The complexes [Cp[∧]RuCl(μ-Cl)]₂⁷ and [Cp[∧]Ru(μ-OMe)]₂^{16c} as well as the substrates **7**,^{22a} **8**,^{22e} **9**,^{23b} **10**,²⁴ and **11**²⁵ were prepared according to published procedures. The following numbering scheme was used for the assignment of the ¹³C NMR data:



[Cp[∧]Ru(μ-OMe)]₂ (**1**). Excess K₂CO₃ (400 mg) was added to a solution of complex [Cp[∧]RuCl(μ-Cl)]₂ (500 mg, 556 μmol) in MeOH (25 mL), and the mixture was stirred for 3 h at 55 °C. During the reaction, the color of the solution changed from brown to orange-red and an orange-red solid appeared. After cooling to room temperature, the solution was filtered and the solid was dried under reduced pressure to remove the MeOH. The product was purified by extraction with hexane and subsequent removal of the solvent under reduced pressure (2 times). The resulting orange solid contains two isomers in the ratio 1:1, which can be distinguished in the ¹H NMR. Yield: 320 mg (70%). ¹H NMR (CD₂Cl₂, 25 °C): δ (ppm) 4.79 (s, 3 H, μ-OCH₃), 4.71 (s, 3 H, μ-OCH₃), 3.67 (s, 3 H, OCH₃, Cp[∧]), 3.63 (s, 3 H, OCH₃, Cp[∧]), 3.24 (s, 1 H, CH), 3.22 (s, 1 H, CH), 2.50 (d, ²*J*_{HH} = 16 Hz, 1 H, CH₂), 2.47 (d, ²*J*_{HH} = 16 Hz, 1 H, CH₂), 2.38 (d, ²*J*_{HH} = 16 Hz, 1 H, CH₂), 2.37 (d, ²*J*_{HH} = 16 Hz, 1 H, CH₂), 1.58 (s, 9 H, *t*-Bu), 1.56 (s, 9 H, *t*-Bu), 1.55 (s, 9 H, *t*-Bu), 1.52 (s, 9 H, *t*-Bu), 0.98 (s, 9 H, *t*-Bu), 0.97 (s, 9 H, *t*-Bu). ¹³C{¹H} NMR (C₆D₅CD₃, 25 °C): δ (ppm) 119.52 (C13), 79.34, 78.61, 73.70, 73.44, 69.55, 69.30 (C10, C11, C12), 57.35, 57.21 (C9, μ-OCH₃), 47.57, 47.39 (C8), 38.90, 38.77 (C7), 34.24, 33.91, 32.19 (C4, C5, C6), 33.44, 33.10, 32.93 (C1, C2, C3). Anal. Calcd for C₄₀H₇₂O₄Ru₂: C, 58.65; H, 8.86. Found: C, 58.87; H, 8.84. Single crystals were obtained from a hexane solution by slow evaporation.

[Cp[∧]Ru(μ-OEt)]₂ (**2**). A small tube containing a hexane solution (4 mL) of complex **1** (500 mg, 610 μmol) was placed in a Schlenk

tube containing EtOH (25 mL). Slow diffusion was allowed at room temperature to give red crystals of complex **2**. The ¹H NMR of **2** showed the presence of two isomers in a ratio of 1:1. Yield: 485 mg (94%). ¹H NMR (CD₂Cl₂, 25 °C): δ (ppm) 4.95 (q, ³*J*_{HH} = 7 Hz, 2 H, μ-OCH₂CH₃), 4.79 (q, ³*J*_{HH} = 7 Hz, 2 H, μ-OCH₂CH₃), 3.61 (s, 3 H, OCH₃, Cp[∧]), 3.53 (s, 3 H, OCH₃, Cp[∧]), 3.33 (s, 1 H, CH), 3.22 (s, 1 H, CH), 2.40 (d, ²*J*_{HH} = 15 Hz, 1 H, CH₂), 2.33 (d, ²*J*_{HH} = 15 Hz, 1 H, CH₂), 1.59 (s, 9 H, *t*-Bu), 1.58 (s, 9 H, *t*-Bu), 1.52 (s, 9 H, *t*-Bu), 1.49 (t, ³*J*_{HH} = 7 Hz, 3 H, μ-OCH₂CH₃), 1.45 (t, ³*J*_{HH} = 7 Hz, 3 H, μ-OCH₂CH₃), 0.96 (s, 9H, *t*-Bu), 0.95 (s, 9H, *t*-Bu). ¹³C{¹H} NMR (C₆D₅CD₃, 25 °C): δ (ppm) 119.25 (C13), 79.86, 79.19, 78.30, 72.02, 70.67, 69.28 (C10, C11, C12), 58.13, 57.93 (C9, μ-OCH₂CH₃), 48.98, 48.73 (C8), 38.35 (C7), 33.87, 33.80, 33.64, 33.57, 32.18 (C4, C5, C6), 33.41, 33.31, 33.01, 32.95, 32.76 (C1, C2, C3), 22.81, 22.72 (μ-OCH₂CH₃). Anal. Calcd for C₄₀H₇₂O₄Ru₂: C, 59.54; H, 9.04. Found: C, 59.41; H, 8.97.

[Cp[∧]Ru(μ-Cl)]₂ (**3**). Excess Me₃SiCl (400 μL) was added to a solution of complex **1** (500 mg, 610 μmol) in THF (25 mL). Subsequent addition of LiCl (100 mg) led to a rapid change in color from orange-yellow to red. The reaction was continued with stirring at 55 °C for 12 h followed by filtration to remove the excess of LiCl. The solvent and the excess Me₃SiCl (bp 57 °C) were removed using a prolonged high vacuum. The residual red solid was extracted with hexane in order to remove remaining lithium salts. The analytically pure product was obtained upon removing the hexane. The ¹H NMR of **3** showed the presence of two isomers in a ratio of 1:2. Yield: 445 mg (88%). ¹H NMR (CD₂Cl₂, 25 °C): δ (ppm) 3.79, 3.77 (s, 1 H, CH), 3.71, 3.68 (s, 3 H, OCH₃, Cp[∧]), 2.84, 2.78 (d, ²*J*_{HH} = 16 Hz, 1 H, CH₂), 2.58, 2.56 (d, ²*J*_{HH} = 16 Hz, 1 H, CH₂), 1.58, *l*.56 (s, 9 H, *t*-Bu), *l*.50, 1.47 (s, 9 H, *t*-Bu), 1.07, *l*.06 (s, 9 H, *t*-Bu). ¹³C{¹H} NMR (CD₂Cl₂, 25 °C): δ (ppm) 122.40, *l*21.94 (C13), 81.42, 80.90, 75.70, 75.46, 74.52, 74.08 (C10, C11, C12), 58.67, 58.61 (C9), 48.02, 47.24 (C8), 38.45, 38.28 (C7), 34.26, 34.12, 33.41, 33.31, 32.28, 32.25 (C4, C5, C6), 33.12, 33.09, 33.07, 33.03, 32.40, 32.35 (C1, C2, C3). The data of the less abundant isomer is shown in italics. Anal. Calcd for C₃₈H₆₆Cl₂O₂Ru₂: C, 55.12; H, 8.03. Found: C, 55.07; H, 8.06. Single crystals were obtained from a solution of the complex in a mixture of MeOH/CH₂Cl₂ at low temperature (-35 °C).

Table 4. Crystallographic Data for Complexes 4 and 5

	4	5
empirical formula	C ₂₆ H ₄₁ BF ₄ Ru	C ₂₃ H ₃₆ O ₅ Ru
mol wt/g mol ⁻¹	541.47	493.59
cryst size/mm ³	0.56 × 0.12 × 0.09	0.41 × 0.21 × 0.19
cryst syst	monoclinic	monoclinic
space group	C2/c	P2 ₁ /c
a/Å	33.840(7)	11.1835(13)
b/Å	8.7777(18)	17.663(2)
c/Å	17.662(4)	12.0386(7)
α /deg	90	90
β /deg	105.54(3)	93.037(7)
γ /deg	90	90
volume/Å ³	5054.6(18)	2374.7(4)
Z	8	4
density/g cm ⁻³	1.423	1.381
temperature/K	100(2)	100(2)
absorp coeff/mm ⁻³	0.661	0.689
θ range/deg	3.40 to 25.02	3.35 to 25.02
index ranges	-40 → 39, -9 → 10, -21 → 21	-13 → 13, -21 → 21, -14 → 14
no. of reflns collected	32819	46627
no. of indep reflns	4439 ($R_{\text{int}} = 0.1178$)	4181 ($R_{\text{int}} = 0.0585$)
absorp corr	semiempirical	semiempirical
max. and min. transm	1.0000 and 0.6482	1.0000 and 0.7924
no. of data/restraints/params	4439/0/289	4181/0/262
goodness-of-fit on F^2	1.131	1.123
final R indices [$I > 2\sigma(I)$]	$R1 = 0.0557$, $wR2 = 0.0903$	$R1 = 0.0257$, $wR2 = 0.0499$
R indices (all data)	$R1 = 0.1121$, $wR2 = 0.1093$	$R1 = 0.0381$, $wR2 = 0.0541$
larg diff peak/hole/e ⁻³	0.758 and -0.559	0.390 and -0.324

[[C₅H₂(*t*-Bu)₂(CH₂-*t*-Bu)]Ru(PhEt)]BF₄ (4). Excess HBF₄ (OEt₂) (70 μ L, 500 μ mol) was added to a solution of complex **1** (100 mg, 122 μ mol) in diethyl ether (10 mL). The color changed from reddish-yellow to pale yellow. Excess cod (60 μ L, 500 μ mol) was then added to the reaction mixture. The solution turned colorless along with the appearance of a white precipitate. The mixture was stirred at room temperature for 12 h followed by filtration. The resulting solid was washed with diethyl ether and dried under high vacuum. Yield: 115 mg (87%). ¹H NMR (CD₂Cl₂, 25 °C): δ (ppm) 6.04–6.13 (m, 5 H, Ph), 5.30 (s, 2 H, CH), 2.73 (s, 2 H, CH₂), 2.52 (q, ³ $J_{\text{HH}} = 8$ Hz, 2 H, PhCH₂CH₃), 1.40 (s, 18 H, *t*-Bu), 1.31 (t, ³ $J_{\text{HH}} = 8$ Hz, 3 H, PhCH₂CH₃), 1.17 (s, 9 H, *t*-Bu). ¹³C{¹H} NMR (CD₂Cl₂, 25 °C): δ (ppm) 115.95, 109.10, 100.06, 95.71 (Ph), 87.60, 85.84, 81.23 (C10, C11, C12), 66.22, 59.25 (C13, C8), 38.66 (C7), 34.90, 34.56, 32.68 (C4, C5, C6), 33.43, 33.30, 33.21 (C1, C2, C3), 28.77 (PhCH₂CH₃), 16.77 (PhCH₂CH₃). Anal. Calcd for C₂₆H₄₁RuBF₄: C, 57.67; H, 7.63. Found: C, 57.28; H, 7.78. White crystals of complex **4** were obtained from a solution of THF and CH₂Cl₂ by slow evaporation.

[Cp[^]Ru(COMe)(CO)₂] (5). Complex **1** (200 mg, 244 μ mol) was dissolved in hexane (10 mL). The nitrogen atmosphere in the Schlenk was replaced by CO at room temperature. A fast reaction took place and the color of the solution changed from orange to yellow. Needle-shaped, yellow crystals of complex **5** appeared from this solution when it was stored at -20 °C. On removing the hexane from the resulting solution, analytically pure product was obtained. Yield: 245 mg (99%). IR: ν (cm⁻¹) 2017, 1957 (CO terminal), 1625 (CO acyl). ¹H NMR (CD₂Cl₂, 25 °C): δ (ppm) 4.83 (s, 1 H, CH), 3.69 (s, 3 H, OCH₃), 3.49 (s, 3 H, COOCH₃), 2.92 (d, ² $J_{\text{HH}} = 16$ Hz, 1 H, CH₂), 2.64 (d, ² $J_{\text{HH}} = 16$ Hz, 1 H, CH₂), 1.45 (s, 9 H, *t*-Bu), 1.41 (s, 9 H, *t*-Bu), 1.16 (s, 9 H, *t*-Bu). ¹³C{¹H} NMR (CD₂Cl₂, 25 °C): δ (ppm) 202.36, 201.95 (CO), 193.66 (COOMe), 147.19 (C13), 113.47, 105.32, 98.90 (C10, C11, C12), 65.33 (C9), 58.54 (C8), 51.80 (COOCH₃), 37.93 (C7), 34.76, 34.35 (C4, C5, C6), 33.69, 33.37, 33.27 (C1, C2, C3). Anal. Calcd for C₂₃H₃₆O₅Ru: C, 55.97; H, 7.35. Found: C, 55.78; H, 7.14. Single crystals were obtained from a hexane solution at low temperature (-20 °C).

General Procedure for ATRC Reactions. Pyridine was added to the desired amount of stock solution of complex **1** in degassed

CD₂Cl₂ or *d*₈-toluene (pyridine/complex **1** = 1.0). The solution was the added to a solution of the substrate containing the internal standard *p*-xylene or 1,4-bis(trifluoromethyl)benzene (final volume = 1000 μ L, [substrate] = 0.15 M, [internal standard] = 50 mM). The resulting solutions were stirred at room temperature or at 60 °C. After a given time, a sample (25 μ L) was removed from the reaction mixture, diluted with CDCl₃ (350 μ L), and analyzed by ¹H NMR spectroscopy.

Crystallographic Investigations. The relevant details of the crystals, data collection, and structure refinement can be found in Tables 3 and 4. Diffraction data were collected using Mo K α radiation on a 4-circle kappa goniometer equipped with a Bruker APEX II CCD at 100(2) K, and all data were reduced by EvalCCD.²⁷ Absorption correction was applied to all data sets using a semiempirical method.²⁸ All structures were refined using the full-matrix least-squares on F^2 with all non-H atoms anisotropically defined. The hydrogen atoms were placed in calculated positions using the "riding model" with $U_{\text{iso}} = aU_{\text{eq}}$ (where a is 1.5 for methyl hydrogen atoms and 1.2 for others). Structure refinement and geometrical calculations were carried out on all structures with SHELXTL.²⁹

Acknowledgment. The work was supported by the Swiss National Science Foundation and by the EPFL. We thank K. Thommes for providing some of the substrates and Dr. E. Solari for help with the crystallographic investigations.

Supporting Information Available: X-ray crystallographic file in CIF format is available free of charge via the Internet at <http://pubs.acs.org>.

OM700992D

(27) Duisenberg, A. J. M.; Kroon-Batenburg, L. M. J.; Schreurs, A. M. M. *J. Appl. Crystallogr.* **2003**, *36*, 220–229.

(28) Blessing, R. H. *Acta Crystallogr., Sect. A* **1995**, *51*, 33–38.

(29) Sheldrick, G. M. *SHELXTL*; University of Göttingen: Göttingen, Germany, 1997; Bruker AXS, Inc.: Madison, WI, 1997.